





Short Research Communication

# Evaluation of a 3-hydroxypyridin-2-one (2,3-HOPO) Based Macrocyclic Chelator for $^{89}\text{Zr}^{4+}$ and Its Use for ImmunoPET Imaging of HER2 Positive Model of Ovarian Carcinoma in Mice

Jeff N. Tinianow<sup>1\*</sup>, Darpan N. Pandya<sup>2\*</sup>, Sylvie L. Pailloux<sup>3</sup>, Annie Ogasawara<sup>1</sup>, Alexander N. Vanderbilt<sup>1</sup>, Herman S. Gill<sup>1</sup>, Simon-P. Williams<sup>1</sup>, Thaddeus J. Wadas<sup>2</sup>, Darren Magda<sup>3</sup>, Jan Marik<sup>1</sup>

1. Department of Biomedical Imaging, Genentech, Inc. 1 DNA way, South San Francisco, CA 94080.
2. Wake Forest School of Medicine, Medical Center Boulevard, Winston-Salem, NC 27157.
3. Lumiphore, Inc. 600 Bancroft Way, Suite B Berkeley, CA 94710.

\*These authors contributed equally to this work.

 Corresponding authors: Jan Marik, Department of Biomedical Imaging, Genentech, Inc., Mailstop 228, 1 DNA Way, South San Francisco, California 94080, USA. Phone: +1 650 225 8821 Fax: +1 650 742 4905 E-mail: [marik.jan@gene.com](mailto:marik.jan@gene.com) Or Darren Magda, Lumiphore, Inc. 600 Bancroft Way, Suite B. Berkeley, CA 94710. [dmagda@lumiphore.com](mailto:dmagda@lumiphore.com).© Ivyspring International Publisher. Reproduction is permitted for personal, noncommercial use, provided that the article is in whole, unmodified, and properly cited. See <http://ivyspring.com/terms> for terms and conditions.

Received: 2015.10.29; Accepted: 2016.01.05; Published: 2016.02.13

## Abstract

A novel octadentate 3-hydroxypyridin-2-one (2,3-HOPO) based di-macrocyclic ligand was evaluated for chelation of  $^{89}\text{Zr}$ ; subsequently, it was used as a bi-functional chelator for preparation of  $^{89}\text{Zr}$ -labeled antibodies. Quantitative chelation of  $^{89}\text{Zr}^{4+}$  with the octadentate ligand forming  $^{89}\text{ZrL}$  complex was achieved under mild conditions within 15 minutes. The  $^{89}\text{Zr}$ -complex was stable *in vitro* in presence of DTPA, but a slow degradation was observed in serum. *In vivo*, the hydrophilic  $^{89}\text{Zr}$ -complex showed prevalently renal excretion; and an elevated bone uptake of radioactivity suggested a partial release of  $^{89}\text{Zr}^{4+}$  from the complex.

The 2,3-HOPO based ligand was conjugated to the monoclonal antibodies, HER2-specific trastuzumab and an isotypic anti-gD antibody, using a p-phenylene bis-isothiocyanate linker to yield products with an average loading of less than 2 chelates per antibody. Conjugated antibodies were labeled with  $^{89}\text{Zr}$  under mild conditions providing the PET tracers in 60-69% yield. Despite the limited stability in mouse serum; the PET tracers performed very well *in vivo*. The PET imaging in mouse model of HER2 positive ovarian carcinoma showed tumor uptake of  $^{89}\text{Zr}$ -trastuzumab ( $29.2 \pm 12.9$  %ID/g) indistinguishable ( $p = 0.488$ ) from the uptake of positive control  $^{89}\text{Zr}$ -DFO-trastuzumab ( $26.1 \pm 3.3$  %ID/g).

In conclusion, the newly developed 3-hydroxypyridin-2-one based di-macrocyclic chelator provides a viable alternative to DFO-based heterobifunctional ligands for preparation of  $^{89}\text{Zr}$ -labeled monoclonal antibodies for immunoPET studies.

Key words: immunoPET, positron emission tomography, monoclonal antibody, imaging,  $^{89}\text{Zr}$ , radiolabeling, 2,3-HOPO, 3-hydroxypyridin-2-one.

## Introduction

Over the last two decades, positron emission tomography (PET) has rapidly become an indispensable tool that is used by pharmaceutical companies to

accelerate therapeutic development. Nowhere is this more easily observed than with the advent of personalized medicine and the expansion of monoclonal

antibodies (mAbs) as targeted therapeutics. PET performed with radiolabeled mAbs (immunoPET) as target specific tracers allows for the whole body assessment of biomarker expression and the non-invasive biodistribution of therapeutic antibodies [1, 2]. Since monoclonal antibodies exhibit a much longer biological half-life than small molecules the most widely used positron emitting radionuclide  $^{18}\text{F}$  ( $T_{1/2} = 110$  min) is not ideal for the radiolabeling of monoclonal antibodies. Zirconium-89 ( $T_{1/2} = 3.3$  d) appears to be the most suitable residualizing radionuclide for immunoPET applications since its decay half-life synergizes with the biological half-life of a monoclonal antibody to provide enough time for the radiolabeled mAb to be cleared from blood pool while allowing sufficient accumulation at the tissue of interest. The decay of chelating  $^{89}\text{Zr}$  to parent  $^{89}\text{Y}$  proceeds by positron emission (22.7%) and electron capture (77.3%). Typically  $^{89}\text{Zr}$  is coupled to the monoclonal antibody through a bifunctional chelator, which consists of a ligand capable of  $^{89}\text{Zr}$  binding and a reactive group that chemoselectively reacts with available lysine or cysteine side chains exposed on the mAb surface. Since  $\text{Zr}^{4+}$  is an extremely hard cation the most suitable ligands for  $^{89}\text{Zr}$  are expected to be anionic oxygen donors [3], and the most widely used chelator for  $^{89}\text{Zr}$ -immunoPET is based on a bacterial siderophore desferrioxamine-B (DFO, **Figure 1A**). This ligand contains a free amino group, which has been easily derivatized to develop a cadre of bifunctional chelators that have been used to prepare  $^{89}\text{Zr}$ -mAbs in numerous pre-clinical and clinical studies [4-6].

Since the hexadentate DFO cannot fulfill the octavalent demands of the  $\text{Zr}^{4+}$  cation, it is not considered ideal for satisfying the coordination sphere of the  $\text{Zr}^{4+}$  cation. Molecular modeling has suggested that the two remaining coordination sites in  $\text{Zr}$ -DFO complex could be occupied with two water molecules [7] leading to kinetic instability of the complex and potential release of the radiometal. Although metabolism studies of  $^{89}\text{Zr}$ -DFO have never been completed, it is believed that the released  $^{89}\text{Zr}$  would bind to plasma proteins, (e.g. transferrin) before being deposited in the bone due to high affinity of  $\text{Zr}^{4+}$  for phosphates [8-10]. Indeed, an increased uptake in mineral bone was observed in all preclinical studies with  $^{89}\text{Zr}$ -labeled antibodies performed in rodents. To mitigate the risk of  $^{89}\text{Zr}$  release, octadentate chelators for  $^{89}\text{Zr}^{4+}$  are being developed in earnest. X-ray crystallographic and molecular modeling studies with  $\text{Zr}^{4+}$  complexed by bidentate hydroxamates suggested higher stability of  $\text{ZrL}_4$  complexes [11], and prompted the development of an octavalent DFO derivative (DFO\*; **Figure 1B**) which was recently prepared by

extending DFO by an additional hydroxamate unit. As predicted by the *in vitro* and *in silico* studies, the stability of  $^{89}\text{Zr}$ -DFO\* was found superior to  $^{89}\text{Zr}$ -DFO [12].

Catecholates, and hydroxypyridinones (HOPO) were also proposed as ligands for  $^{89}\text{Zr}$  chelation [3, 11, 13]. HOPO based chelators were developed as actinide sequestration agents for chelation therapy [14, 15] and some were used for chelating  $\text{Gd}^{3+}$  as a contrast agent for MRI imaging [16]. The recent evaluation of 1-hydroxypyridin-2-one based chelator 3,4,3-(LI-1,2-HOPO) (**Figure 1C**) led to the successful preparation of the  $^{89}\text{Zr}$  complex. It's *in vitro* stability was superior to  $^{89}\text{Zr}$ -DFO [13], and small animal PET imaging demonstrated its hepatobiliary clearance, which is in contrast to the rapid renal clearance of  $^{89}\text{Zr}$ -DFO. However, observed bone uptake in mice injected with  $^{89}\text{Zr}$ -3,4,3-(LI-1,2-HOPO) was higher than the bone uptake in mice receiving  $^{89}\text{Zr}$ -DFO. The authors attributed the elevated uptake in bone to a slower hepatobiliary clearance and longer residence time of  $^{89}\text{Zr}$ -3,4,3-(LI-1,2-HOPO) in circulation than  $^{89}\text{Zr}$ -DFO. Indeed, the subsequent *in-vivo* study conducted with  $^{89}\text{Zr}$ -3,4,3-(LI-1,2-HOPO)-trastuzumab showed lower bone uptake compared to  $^{89}\text{Zr}$ -DFO-trastuzumab [17].

Additionally Ma *et al.* reported the use of  $\text{H}_3\text{CP256}$ , a tris(hydroxypyridinone) ligand containing 1,6-dimethyl-3-hydroxypyridin-4-one chelating units and its bifunctional chelator analogue YM103, which contained a maleimide group engineered into the ligand scaffold for facile site specific modifications of antibodies through available, active cysteine residues [18]. While  $^{89}\text{Zr}$ -CP256 (**Figure 1D**) was observed to be highly stable *in vitro* and *in vivo*, the stability of  $^{89}\text{Zr}$ -YM103-trastuzumab was far less robust. Both acute biodistribution studies and small animal PET imaging revealed an approximate 3-fold increase of radioactivity in the bones of animals injected with  $^{89}\text{Zr}$ -YM103-trastuzumab when compared to the bones of animals injected with  $^{89}\text{Zr}$ -DFO-trastuzumab. These results led the authors to conclude that the acyclic, tripodal arrangement of the hydroxypyridinone groups in  $\text{H}_3\text{CP256}$  and YM103 were not optimal for the enhanced kinetic stability of the respective  $^{89}\text{Zr}$  complexes where prolonged *in vivo* stability was required.

In this paper, we describe the preparation and evaluation of octadentate chelators containing 3-hydroxypyridin-2-one coordinating units (BPDET-LysH22-2,3-HOPO (**1**); **Figure 1E**) and its mAb conjugate. The novel "clam shell" design of the bi-macrocyclic chelator **1** was chosen as a compromise between a linear geometry of DFO-like siderophores and rigid macrocyclic geometry to allow for fast che-

lation of the metal and providing stability of the resulting complex. The free amino group of **1** was derivatized with p-phenylene bis-isothiocyanate to provide an amino-reactive linker for conjugation to monoclonal antibodies via lysine side chains (**Figure 1F**).

Two antibodies, trastuzumab and anti-gD, were conjugated with **1** and chelated with  $^{89}\text{Zr}$  and their *in vivo* PET imaging properties were compared to the same pair of antibodies labeled by DFO. The mouse model of HER2 positive human ovarian carcinoma (SKOV3) was chosen to compare HER2-specific uptake of  $^{89}\text{Zr}$ -trastuzumab labeled by **1** and DFO. An isotopic antibody binding to glycoprotein D (gD) was also labeled with  $^{89}\text{Zr}$  using **1** and DFO and used as a negative control to estimate non-specific uptake.

## Materials and Methods

### General

Zirconium-89 ( $^{89}\text{Zr}$ ) was purchased from Washington University School of Medicine (St. Louis, MO), IBA Molecular, Inc. (Dulles, VA) or Perkin-Elmer (Waltham, MA) as  $^{89}\text{Zr}^{4+}$  oxalate ( $^{89}\text{Zr}(\text{Ox})_2$ ) in 1M oxalic acid solution. Unless otherwise noted, all other chemicals were purchased from Sigma-Aldrich Chemical Co. (St. Louis, MO USA), and solutions were prepared using ultrapure water (18 M $\Omega$ -cm resistivity). Anti-human epidermal growth factor receptor 2 (HER2) antibody trastuzumab and the isotopic (IgG1) control anti-gD antibody (anti-glycoprotein D) were produced at Genentech Inc.

and stored in 0.01 M sodium acetate, 240 mM sucrose, 0.02% polysorbate 20, pH 5.5. NAP-10 columns were obtained from GE Healthcare (Piscataway, NJ) and Amicon Ultra-4 centrifugal filters (10,000 MWCO) from Millipore (Billerica, MA).  $^{\text{Nat}}\text{Zr}$ -DFO and  $^{89}\text{Zr}$ -DFO were synthesized according to a previously published procedures [19].

### Analytical Chemistry

Electrospray ionization (ESI) high-resolution mass spectra (HRMS) were obtained by the Mass Spectrometry Facility, College of Chemistry, University of California, Berkeley, CA. Flash chromatography was performed using EM Science Silica Gel 60 (230 - 400 mesh). NMR spectra were obtained using either Bruker AM-300 or AV-600 spectrometers operating at 300 (75) MHz and 600 (150) MHz for  $^1\text{H}$  (or  $^{13}\text{C}$ ) respectively.  $^1\text{H}$  (or  $^{13}\text{C}$ ) chemical shifts are reported in parts per million (ppm) relative to the solvent resonances, taken as  $\delta$  7.26 ( $\delta$  77.0) for  $\text{CDCl}_3$ . For the deprotected macrocycles **1** and **2** (**Scheme S1**), the observed NMR spectra were very complicated due to the presence of differing conformers/isomers in solution, and are not reported. Analytical HPLC was performed on an Agilent 1200 instrument (Agilent, Santa Clara, CA) equipped with a diode array detector ( $\lambda = 280$  or 315 nm, 600 nm reference), a thermostat set at 25  $^\circ\text{C}$ , and a Zorbax Eclipse XDB-C18 column (4.6  $\times$  150 mm, 5  $\mu\text{m}$ , Agilent, Santa Clara, CA). The mobile phase of a binary gradient (Method 1: 2-40% B in 20 min; solvent A, 0.1% TFA; solvent B, ACN or Method 2: 10-60% B; 20 min) at a flow rate of 1 mL/min was

used for analytical HPLC. All compounds were  $\geq 95\%$  pure if not stated otherwise.

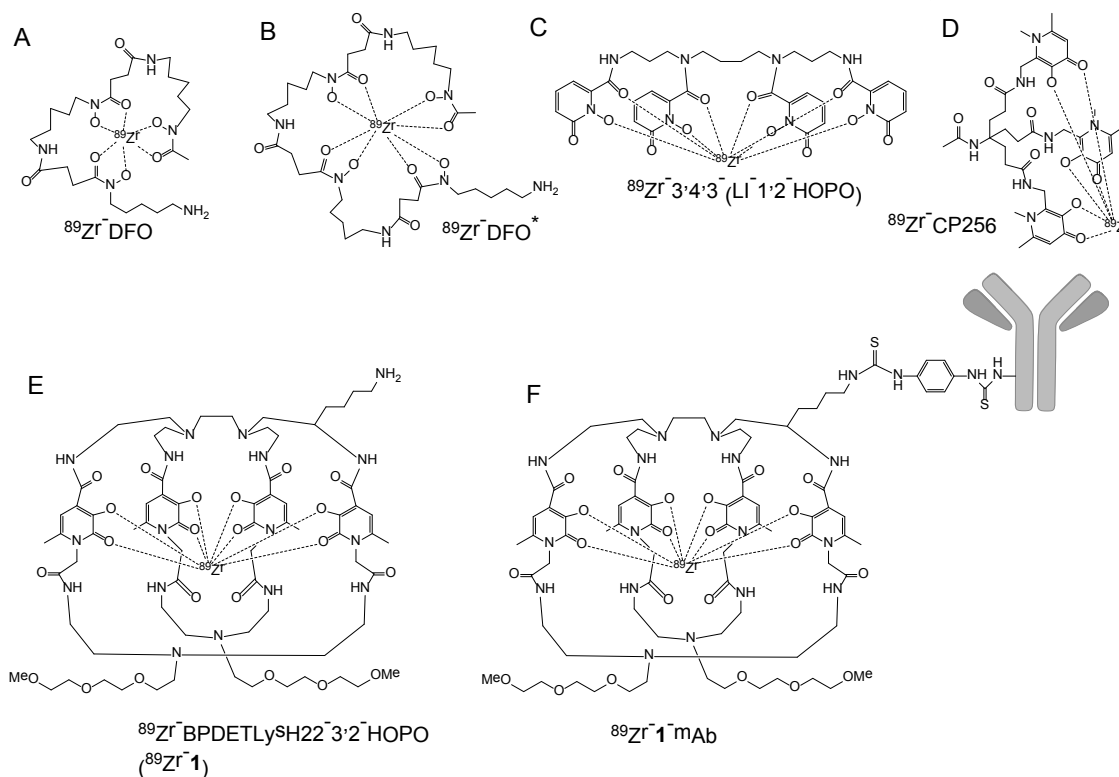


**Figure 1.** Bifunctional chelators for  $^{89}\text{Zr}$  and their proposed modes of  $^{89}\text{Zr}$  binding.

Determination of antibody loading with DFO was performed on a Agilent 1200 Series LC with PLRP-S, 1000 Å, column (50 mm × 2.1 mm, Varian Inc., Palo Alto, CA) coupled to an Agilent 6220 Accurate-Mass TOF LC/MS mass spectrometer (Santa Clara, CA). A linear gradient from 34–45% B in 5 min (solvent A, 0.1% formic acid in water; solvent B, 0.1% formic acid in acetonitrile, 0.5 mL/min) was employed with direct injection of the eluent to an electrospray ionization source. Protein concentrations were measured at 280 nm using Eppendorf BioPhotometer (Westbury, NY).

### Surface Plasmon Resonance Spectroscopy

DFO- and **1**-conjugated trastuzumab (20 µg/mL) were amine coupled to independent channels of a carboxylate sensor surface (COOH<sub>2</sub>, Snsiq Technologies Inc., Oklahoma City, OK). Serial two-fold dilutions of HER2 extracellular domain antigen were prepared from 50 to 0.2 nM concentration in running buffer containing PBS with 0.02% Tween-20 and were injected across each channel from which the affinity ( $K_D$ ) was determined by a global fit of  $k_{on}$  and  $k_{off}$  at each concentration.

### Analytical Radiochemistry

Radiochemistry reaction progress and purity were analyzed by using a Waters analytical HPLC (Milford, MA), which runs Empower software and is configured with a 1525 binary pump, 2707 autosampler, 2998 photodiode array detector, 2475 multichannel fluorescence detector, 1500 column heater, fraction collector, Grace Vydac 218MS C18 column (5 µm, 4.6 × 250 mm, Grace Davidson, Deerfield, IL) and a Carrol Ramsey 105-s radioactivity detector (Berkeley, CA). All ligands (DFO, **1**) and associated <sup>Nat</sup>Zr-complexes were monitored at 220 nm using a mobile phase consisting of 0.01% TFA/H<sub>2</sub>O (solvent A) and 0.01% TFA/acetonitrile (solvent B), and a gradient consisting of 0% B to 70% B in 20 min at a flow rate of 1.2 mL/min. In addition, radio-TLC was conducted on a Bioscan AR 2000 radio-TLC scanner equipped with a 10% methane:argon gas supply and a PC interface running Winscan v.3 analysis software (Eckert & Ziegler, Berlin, DE). Varian ITLC-SG strips were employed using a 50 mM DTPA (pH 7) solution as eluent, and the complex <sup>89</sup>Zr(Ox)<sub>2</sub> as a standard control. Radioactive samples were counted using a Perkin Elmer 2480 Wizard<sup>®</sup> gamma counter (Waltham, MA; energy window of 500–1500 keV) and standard protocols [19].

The radiochemical purity of <sup>89</sup>Zr-Df-mAbs was determined by SEC HPLC on Agilent 1200 series LC system equipped with radiation and UV detectors using TOSOH Biosciences TSKgel G3000SW (7.8 mm

× 30 cm × 5 µm), 200 mM sodium phosphate 250 mM sodium chloride, 15% isopropanol pH 7.2 was used as a mobile phase at 0.8 mL/min.

### Animal models

All animal experiments were conducted in compliance with Institutional Animal Care and Use Committee guidelines established by Wake Forest University Health Science's or Genentech's Institutional Animal Care and Use Committee. Both are accredited by the Association for Assessment and Accreditation of Laboratory Animal Care (AAALAC). Female NIH Swiss mice (weight, 20–22 g; age, 6–8 weeks) were obtained from Jackson Laboratories (Bar Harbor, ME). NCR nude mice of age 10 weeks were obtained from Taconic (Oxnard, CA). Mice were inoculated on the right flank with 5 × 10<sup>6</sup> SKOV3 cells (ATCC, Manassas, VA) in a 50:50 ratio of HBSS and phenol red free Matrigel (BD Biosciences, San Jose, CA). Tumor growth was evaluated manually with calipers on a weekly basis. Tumor volume was calculated using a standard formula (volume = 0.52 × [width]<sup>2</sup> × [length]).

### Synthesis of BPDETLysH22-2,3-HOPO (I)

Bifunctional 3,2-HOPO chelator **1** was prepared under high dilution conditions from tetra-amine and active di-amide precursors followed by acid deprotection. The phenylisothiocyanate derivative **1**-NCS was prepared by reaction with p-phenylene bis-isothiocyanate. Further details are described in the **Supporting Information**.

### Synthesis of <sup>Nat</sup>Zr-1

To a solution of **1** (0.5 mg, 0.31 µmol) and ZrCl<sub>4</sub> (0.11 mg, 0.46 µmol) in 0.5 mL of water was added 0.1 M Na<sub>2</sub>CO<sub>3</sub> to adjust pH 7–7.5. The resulting solution was stirred for 1 h at room temperature. Then the mixture was lyophilized to give a white solid. Formation of <sup>Nat</sup>Zr-**1** complex was confirmed by ESI-MS analysis. Calculated for C<sub>72</sub>H<sub>107</sub>N<sub>17</sub>O<sub>22</sub>Zr, 826.83 [(MH<sub>2</sub>)<sup>+2</sup>] Found: 826.83 [(MH<sub>2</sub>)<sup>+2</sup>].

### Synthesis of <sup>89</sup>Zr-1

The complexation of <sup>89</sup>Zr with **1** was achieved by reacting 10 µg (10 µL, 1.0 mg/mL in water) of **1** with an aliquot of <sup>89</sup>Zr(Ox)<sub>2</sub> (22.2 MBq) that was diluted in 100 µL of water and pH adjusted to 7–7.5 using 1 M Na<sub>2</sub>CO<sub>3</sub>. The reactions were incubated at 24°C for 15 min in a thermomixer (550 rpm). Formation of <sup>89</sup>Zr-**1**, was monitored by radio-TLC using Varian ITLC-SG strips and 50 mM DTPA (pH 7) as the mobile phase. In this system, free <sup>89</sup>Zr forms a complex with DTPA and is eluted with the solvent front, while <sup>89</sup>Zr-**1** remains at the origin. The identity of each radioactive complex was further confirmed by comparing its ra-

dio-HPLC elution profile to the UV-HPLC spectrum of  $^{89}\text{Zr}$ -1.

### **In vitro serum stability and DTPA challenge study**

*In vitro* stability was carried out by adding 10  $\mu\text{L}$  of each  $^{89}\text{Zr}$ -labeled complex (1.85 MBq) to 500  $\mu\text{L}$  DTPA (50 mM, pH 7), or human serum. The solutions ( $n = 12$ ) were incubated at 37°C for 7 days and were analyzed daily for 1 week by radio-TLC using Varian IITLC-SG strips and 50 mM DTPA (pH 7) as the mobile phase and gamma counting using an energy window of 500-1500 keV and standard protocols [19].

### **Determination of partition coefficients (logP).**

The partition coefficient (LogP) for each complex was determined by adding 5  $\mu\text{L}$  of each  $^{89}\text{Zr}$ -labeled complex (approx. 0.2 MBq) to a mixture of 500  $\mu\text{L}$  of octanol and 500  $\mu\text{L}$  of water. The resulting solutions ( $n = 4$ ) were vigorously vortexed for 5 min at room temperature, then centrifuged at 17,000 rpm for 5 min to ensure complete separation of layers. From each of the four sets, 50  $\mu\text{L}$  aliquot was removed from each phase into screw tubes and counted separately in a gamma counter. Each organic phase was washed with water to remove any radioactivity remaining in the organic phase before gamma counting. The partition coefficient was calculated as a ratio of counts in the octanol fraction to counts in the water fraction.

### **Biodistribution Studies**

Biodistribution studies were conducted using a modified literature procedure [20]. Briefly, female NIH Swiss mice (6-8 weeks old,  $n = 6$ ) were injected with each  $^{89}\text{Zr}$ -labeled complex (0.5 MBq per mouse) via the tail vein, and sacrificed at 2, 4, 24, 48, 72 h post injection (p.i.). Organs and tissues of interest were excised, weighed, and radioactivity was measured on a Perkin Elmer 2480 Wizard<sup>®</sup> gamma counter (Waltham, MA). The percent injected dose per gram (%ID/g) and percent injected dose per organ (%ID/organ) were calculated by comparison to a weighed, counted standard for each group.

### **Synthesis of 1-trastuzumab and 1-gD**

The 5 mM stock solution of the bifunctional chelator was prepared by dissolving 1-NCS (2.62 mg, 1.5 mmol) in DMF (0.3 mL), the stock solution was then aliquoted and frozen at -20°C. The mAb solution was buffer exchanged into 50 mM sodium acetate pH 8.5 using a NAP-10 column. An aliquot of the 1-NCS stock solution (87  $\mu\text{L}$ , 0.42  $\mu\text{mol}$ ; a 6-fold molar excess) was then added to the solution of antibody (10.7 mg, 0.07  $\mu\text{mol}$ ) in 50 mM sodium acetate pH 8.5 (0.8 mL) and incubated at 37°C for 90 minutes. The reaction was stopped by buffer exchange on a NAP-10 into

0.01 M sodium acetate, 240 mM sucrose, 0.02% polysorbate 20, pH 5.5 (1.5 mL). The average loading (chelator/antibody ratio) was determined by mass spectrometry.

### **Synthesis of $^{89}\text{Zr}$ -1-mAb and $^{89}\text{Zr}$ -DFO-mAb**

The solution of  $^{89}\text{Zr}(\text{Ox})_2$  (74-150 MBq, 100  $\mu\text{L}$ ) in 1 M oxalic acid was mixed with 2 M solution of  $\text{K}_2\text{CO}_3$  (50  $\mu\text{L}$ ) and incubated at room temperature for 3 min after which 0.5 M HEPES buffer pH 7 (650  $\mu\text{L}$ ) was added. Then 200  $\mu\text{L}$  of mAb-conjugate (1 mg, 7 nmol) was added to the  $^{89}\text{Zr}$  solution providing a total volume of 1 mL. The mixture was incubated at room temperature for 1 h. To remove non-chelated  $^{89}\text{Zr}^{4+}$  the radiolabeled protein was purified using a NAP-10 desalting column pre-equilibrated with 20 mL of the elution buffer. The reaction mixture was loaded on the column and the  $^{89}\text{Zr}$ -mAb was eluted with 0.01 M sodium acetate, 240 mM sucrose, 0.02% polysorbate 20, pH 5.5 buffer (1.5 mL). If the purified chelate contained radioactive low molecular weight species, the  $^{89}\text{Zr}$ -mAb was further purified using an Amicon Ultra-4 filter (10K).

### **Determination of *in vitro* $^{89}\text{Zr}$ -mAb stability in mouse serum**

A solution of  $^{89}\text{Zr}$ -1-trastuzumab conjugate in 20 mM sodium succinate and 240 mM sucrose, pH 5.5 (0.2-0.4 mL) was added to fresh mouse serum (0.7 mL) and incubated at 37°C for 0-96 h. Samples (70  $\mu\text{L}$ ) of the serum solution were analyzed using SEC HPLC.

### **PET imaging**

Mice ( $n = 5$  per group) were injected via the lateral tail vein with approximately 3.7 MBq of  $^{89}\text{Zr}$ -mAb (5 mg/kg mAb) in 100  $\mu\text{L}$  of 0.9% saline and imaged 1 hour, 1 day, 3 days, and 6 days p.i. of tracer. PET imaging was conducted using Siemens Inveon MM PET/CT scanners (Siemens Preclinical Solutions, Knoxville, TN, USA). Animals were lightly anesthetized with approximately 3.5% sevoflurane for restraint, and body temperature was maintained at 37°C by warm air flow. PET data were acquired as 15 minute static scans for time points at 2 days p.i. and earlier, and increased to 30 minutes for day 6 scans to compensate for radioactive decay. All PET scans were immediately followed by CT scans for anatomical reference and attenuation correction of PET data. List mode data were reconstructed into images with 128  $\times$  128 in-plane voxels of 0.4  $\times$  0.4 mm and 0.8 mm through-plane voxel thickness using vendor-provided iterative OP-MAP implementation with the hyperparameter  $\beta$  set to 0.05 [21].

## Image Analysis

Region of interest (ROI) measurements were performed on multiple axial slices of the tissues using IRW software (Siemens Preclinical Solutions, Knoxville, TN, USA). Decay-corrected signal intensity of tumor and mediastinal blood pool, was measured as percentage of the injected dose per gram (%ID/g), assuming a tissue density of 1 g/cm<sup>3</sup>.

## Statistical Analysis

All of the data are presented as mean  $\pm$  SD or mean (95% Confidence Interval), and statistical classifications were performed using a student's t test (two-tailed, unpaired). Statistical analysis was performed with R software version 3.0.2 (R Foundation for Statistical Computing, Vienna, Austria) or GraphPad Prism (San Diego, CA). Any  $p < 0.05$  was considered significant.

## Results and Discussion

The goal of this work was to evaluate ligand **1** as a novel chelator for <sup>89</sup>Zr immuno-PET applications. While similar systems have been suggested as efficient actinide sequestration agents or as chelates for <sup>89</sup>Zr [13, 22, 23], the ligand described in this report incorporates 3,2-HOPO coordinating units into a larger di-macrocyclic motif since it is widely accepted that the structural rigidity of the macrocyclic framework will impart additional stability to the resulting radiometal complex that cannot be achieved in acyclic ligands [24]. An additional design feature of this ligand includes the incorporation of an amine functionalized pendant arm that provides an available site for facile bioconjugation to proteins, antibodies, peptides or nanoparticles. The synthesis of this ligand involves the condensation of the tetraamine and activated di-acid intermediates under high dilution conditions, followed by chromatography to yield **1**, and further details of the synthesis are provided in the **Supporting Information**. Additionally, the nonradioactive <sup>Nat</sup>Zr-**1** was prepared by reacting **1** with a slight excess of ZrCl<sub>4</sub> (1.5 equiv.) in water under neutral conditions for 1 h at room temperature, and HPLC analysis of the reaction demonstrated that the product had a retention time of 9.3 minutes, which is similar to that of the free ligand (9.1 minutes, **Figure S2**). Interestingly, <sup>Nat</sup>Zr-**1** demonstrated a broadened peak shape in the HPLC chromatogram, which is attributed to the presence of structural isomers. Although ESI-MS analysis of <sup>Nat</sup>Zr-**1** confirmed the 1:1 binding of Zr<sup>4+</sup> to **1** (**Figure S1**), the presence of isomers is entirely reasonable given the available coordination motifs that ligand **1** may make available to the Zr<sup>4+</sup> ion in solution.

Initial radiochemical studies focused on opti-

mizing reaction conditions such as time, temperature, and pH for the efficient and quantitative labeling of **1** with <sup>89</sup>Zr. These investigations revealed that **1** could be quantitatively radiolabeled with <sup>89</sup>Zr within 15 minutes at ambient temperature suggesting this ligand exhibits <sup>89</sup>Zr binding characteristics that are similar to other HOPO and terephthalamide (TAM) ligands reported in the literature [19]. Radio-HPLC analysis revealed that <sup>89</sup>Zr-**1** exhibited a peak profile similar to that of <sup>Nat</sup>Zr-**1** and had a retention time of 9.9 minutes. The specific activity (A<sub>s</sub>) for <sup>89</sup>Zr-**1** was observed to be 0.9 GBq/μmol, and represents an achievable yield that is in agreement with the A<sub>s</sub> of similar <sup>89</sup>Zr-complexes [13, 19].

Lipophilicity (LogP), is an important criterion that yields insight into the adsorption, distribution, metabolism, and elimination of <sup>89</sup>Zr-complexes *in vivo* and was determined using a water/octanol partition [25-28]. Although there are many ways to assess a molecule's lipophilicity, a water-octanol experimental model was chosen since it accurately reflects the true partitioning behavior of all species present in each layer. Based upon the results of these studies, <sup>89</sup>Zr-**1** demonstrates a LogP value of  $-1.53 \pm 0.03$ , which indicates hydrophilic character, and is most likely due both to charge and the numerous hydrogen bonding motifs this complex presents in solution. While this value suggests that renal excretion would be a preferred route of elimination after *in vivo* injection, it is interesting to note that the LogP value of this complex at neutral pH is much more positive than that of <sup>89</sup>Zr-DFO ( $-2.83 \pm 0.04$ ) or <sup>89</sup>Zr-complexes involving di-macrocyclic terephthalamide ligands, which have been recently described in the literature [19].

Although Zr has no known role in biological systems, the uncontrolled release of <sup>89</sup>Zr from injected radiopharmaceuticals due to transchelation remains a major concern since Zr's high affinity for phosphorus leads to its eventual deposition into phosphate rich tissues including the liver, kidney and bone [29-31]. Therefore, understanding the stability of <sup>89</sup>Zr chelates alone or as part of a radiopharmaceutical is critically important. Accordingly, the stability of <sup>89</sup>Zr-**1** was assessed *in vitro* by challenging the radiometal chelate with 50 mM DTPA solution or human serum over the course of seven days at 37°C, and these results are described in **Table S1** and **Table S2**, respectively. Under the experimental conditions described, <sup>89</sup>Zr-**1** was observed to be more resistant to DTPA challenge than <sup>89</sup>Zr-DFO over the seven-day study. After 24 h and 168 h, the amount of <sup>89</sup>Zr initially complexed to DFO was reduced by 45% and 59%, respectively, while under similar conditions <sup>89</sup>Zr-**1** experienced 0% and 22% trans-chelation, respectively. While the stability of <sup>89</sup>Zr-**1** was not as impressive as ligands re-

ported with similar coordinating motifs [19], the data suggests that the HOPO ligand is vastly superior to DFO in this context. However, stability of  $^{89}\text{Zr-1}$  in serum appeared to be far less impressive, and suggests a discrepancy between the DTPA and serum stability results. While transchelation is one possible explanation for this discrepancy, another explanation could be the binding of intact complex to serum proteins through hydrophobic interactions, and further efforts to characterize these interactions are currently underway.

To assess the global retention and clearance of  $^{89}\text{Zr-HOPO}$  *in vivo*, biodistribution studies were conducted in normal mice and the results of those studies are described in **Table S3**. By 72 h p.i.,  $^{89}\text{Zr-1}$  demonstrated comparable blood clearance to  $^{89}\text{Zr-DFO}$  ( $^{89}\text{Zr-DFO}$  vs  $^{89}\text{Zr-1}$ ) (blood,  $0.000 \pm 0.001$  %ID/g vs.  $0.003 \pm 0.002$  %ID/g). However, liver and kidney retention remained elevated ( $^{89}\text{Zr-DFO}$  vs  $^{89}\text{Zr-1}$ ) (liver,  $0.07 \pm 0.01$  %ID/g vs.  $0.43 \pm 0.03$  %ID/g; kidney,  $0.69 \pm 0.09$  %ID/g vs.  $14.73 \pm 2.20$  %ID/g). The elevated retention of radioactivity in these tissues may reflect several active mechanisms either alone or in concert. For example, elevated retention may result from radiometal complex aggregation or protein binding. Additionally, acid decomplexation, trans-chelation and precipitation caused by lysosomal degradation within cells may also be the cause of the increased radioactivity retention in these tissues. While the nature of the radioactive species is unknown, metabolism studies are currently underway to elucidate whether this retention results from complex aggregation, protein transchelation or  $^{89}\text{Zr}$  precipitation *in situ*.

The affinity of  $^{89}\text{Zr}$  for hydroxylapatite, the phosphate-rich molecule found in bone is well documented [29]. Accordingly the amount of  $^{89}\text{Zr}$  retained in bone after  $^{89}\text{Zr}$ -radiopharmaceutical injection remains a critical metric for determining the utility of new  $^{89}\text{Zr}$  chelators. Biodistribution studies involving  $^{89}\text{Zr-1}$  revealed that animals injected with this radiometal complex had more radioactivity retained in their bones than did animals receiving  $^{89}\text{Zr-DFO}$  ( $^{89}\text{Zr-DFO}$ :  $0.08 \pm 0.01$  %ID/g vs.  $^{89}\text{Zr-1}$ :  $0.28 \pm 0.08$  %ID/g). Similar studies using an acyclic HOPO ligand architecture also revealed elevated bone retention when compared to DFO, but the true utility of any ligand containing HOPO coordinating units will only be understood once this ligand type is radiolabeled as part of an antibody based radiopharmaceutical [13].

After the evaluation of the radiometal chelate, the performance of **1** as part of a mAb conjugate was evaluated. Accordingly, the amino reactive heterobifunctional chelator **1-NCS** was prepared by reacting **1** with p-phenylene bis-isothiocyanate linker. The con-

jugation of **1-NCS** to antibodies (HER2 specific trastuzumab and a control antibody binding gD) was achieved by 90 minutes long incubation of antibody with 6-fold excess of **1-NCS** at pH 8.5. The progress of the conjugation was monitored by LCMS and the final loading was determined by mass spectrometry. The reaction yielded monoclonal antibodies covalently modified with 1.7 molecules of **1**. The DFO-trastuzumab and DFO-gD were obtained with loading of 1.3 and 1.4 molecules of DFO per antibody according to previously published procedure using  $\text{Fe}^{3+}$  protected activated ester TFP-NSucDFO-Fe [6]. The binding of **1-trastuzumab** and DFO-trastuzumab to the extracellular domain of HER2 was determined by SPR, and both (0.50 nM and 0.48 nM, respectively), were in very good agreement with the binding affinity of non-modified trastuzumab ( $0.5 \pm 0.1$  nM) [32].

The antibodies conjugated with **1** or DFO were labeled with  $^{89}\text{Zr}$  using the same protocol. The  $^{89}\text{Zr-DFO-mAbs}$  were obtained in 83% and 79% yields, respectively and both had radiochemical purities greater than 95%,  $^{89}\text{Zr-1-trastuzumab}$  and  $^{89}\text{Zr-1-gD}$  were obtained in 60% and 69% yields, respectively. The purity of  $^{89}\text{Zr-1-trastuzumab}$  and  $^{89}\text{Zr-1-gD}$  was greater than 90% by UV, but it was lower as determined by radioactivity detector, 81% and 64% respectively. The impurities present in both tracers labeled with **1** were observed as radioactive low and high molecular weight species, which could not be separated from the radiolabeled mAbs and could not be further characterized (**Figure S3**). Specific activities of  $^{89}\text{Zr-1-mAbs}$  were 30 and 33 MBq/mg and the specific activities of  $^{89}\text{Zr-DFO-mAbs}$  were 41 and 44 MBq/mg. The data is summarized in **Table S4**.

To assess the stability of  $^{89}\text{Zr-1-trastuzumab}$ , the tracer was incubated in mouse serum at  $37^\circ\text{C}$  for four days and the amount of intact  $^{89}\text{Zr-1-trastuzumab}$  was monitored by SEC HPLC. The amount of intact, non-aggregated material in the mouse serum quickly dropped to approximately 50% within first 24 hours then the rate of the loss of the parent material slowed and stabilized around 40% (**Figure S4**). Similar serum stability profile was observed with the non-conjugated  $^{89}\text{Zr-1}$  complex although the amount of remaining intact  $^{89}\text{Zr-1}$  was close to 90% (**Table S2**). The products of  $^{89}\text{Zr-1-trastuzumab}$  decomposition in mouse serum were observed to be high molecular weight aggregates (40%) while the remaining 20% was attributed to low molecular weight species.

The *in vivo* PET imaging properties of  $^{89}\text{Zr-1-trastuzumab}$  and  $^{89}\text{Zr-1-gD}$  were compared to the same antibodies labeled using  $^{89}\text{Zr-DFO}$ . A mouse model of HER2 over-expressing ovarian cancer (SKOV3) was chosen to compare the ability of each

radiotracer to visualize HER2 positive tumors. The isotopic antibody binding to glycoprotein D from HSV virus (gD) was used as a negative control to estimate non-specific uptake of the tracers as the antigen is absent in mammalian tissue.

The time activity curves for tumor, blood, liver and bone obtained during PET imaging are shown at **Figure 2A**. The blood pool levels of all tracers measured in the region of interest encompassing the left ventricle were in the range 25-30 %ID/g at 1 h p.i., the value is typical for pre-clinical immunoPET experiments in mice. The only notable difference observed at 1 h p.i. was the elevated liver uptake of **1**-labeled antibodies compared to  $^{89}\text{Zr}$ -DFO-labeled conjugates. The liver uptake of  $^{89}\text{Zr}$ -**1**-trastuzumab ( $22.3 \pm 2.4$  %ID/g) was comparably higher than the uptake of  $^{89}\text{Zr}$ -DFO-trastuzumab  $16.1 \pm 3.5$  %ID/g ( $p = 0.0007$ ). The liver uptake of  $^{89}\text{Zr}$ -**1**-labeled anti-gD reached similar values with  $^{89}\text{Zr}$ -**1**-gD trending higher than DFO-gD ( $p = 0.053$ ). The elevated liver uptake of tracers labeled with **1** within the first hour p.i. could be attributed to presence of high molecular weight aggregates and lower molecular weight lipophilic impurities in  $^{89}\text{Zr}$ -**1**-trastuzumab and  $^{89}\text{Zr}$ -**1**-gD (**Table S4**, **Figure S3**).

Statistically significant differences in retention of the four tracers in the tumor were apparent at 24 h p.i. The tumor uptake of both trastuzumab derived tracers (**Figure 2A**) was higher than the retention of their anti-gD counterparts ( $p = 0.0014$  for DFO-tracers, and

$p = 0.0006$  for tracers labeled with **1**) and no difference in tumor uptake was observed between  $^{89}\text{Zr}$ -DFO-trastuzumab and  $^{89}\text{Zr}$ -**1**-trastuzumab. At day 3 p.i. this trend continued while the most pronounced differences were observed after 6 days. At day 6 p.i., the average tumor uptake in the group imaged with  $^{89}\text{Zr}$ -**1**-trastuzumab was  $29.2 \pm 12.9$  %ID/g and the tumor uptake in the group imaged with  $^{89}\text{Zr}$ -DFO-trastuzumab was  $26.1 \pm 3.3$  %ID/g, the difference between groups was not statistically significant ( $p = 0.488$ ). The uptake of the isotopic control antibodies  $^{89}\text{Zr}$ -DFO-gD and  $^{89}\text{Zr}$ -**1**-gD in the tumor tissue was  $9.2 \pm 2.0$  %ID/g and  $6.0 \pm 0.6$  %ID/g. The non-specific uptakes of anti-gD antibodies in the tumor were significantly lower than the HER2-specific tumor uptakes of trastuzumab derived tracers,  $p = 0.001$  for DFO chelator and  $p = 5.7 \times 10^{-5}$  for **1** respectively. The non-specific uptakes of  $^{89}\text{Zr}$ -**1**-gD and  $^{89}\text{Zr}$ -DFO-gD in the tumor were not statistically different ( $p = 0.468$ ).

A faster clearance of tracers labeled with **1** from blood pool was apparent at 24 h p.i. (**Figure 2B**). The blood pool uptake of tracers employing **1** was significantly lower than the uptake of DFO-tracers ( $p = 0.023$  for trastuzumab pair and  $p = 0.012$  for gD pair). The trend continued through day 3; at day 6, the blood pool uptake was significantly higher for DFO-conjugated antibodies than for **1**-conjugated antibodies ( $p = 0.0006$  for gD pair, and  $p = 0.003$  for trastuzumab pair).

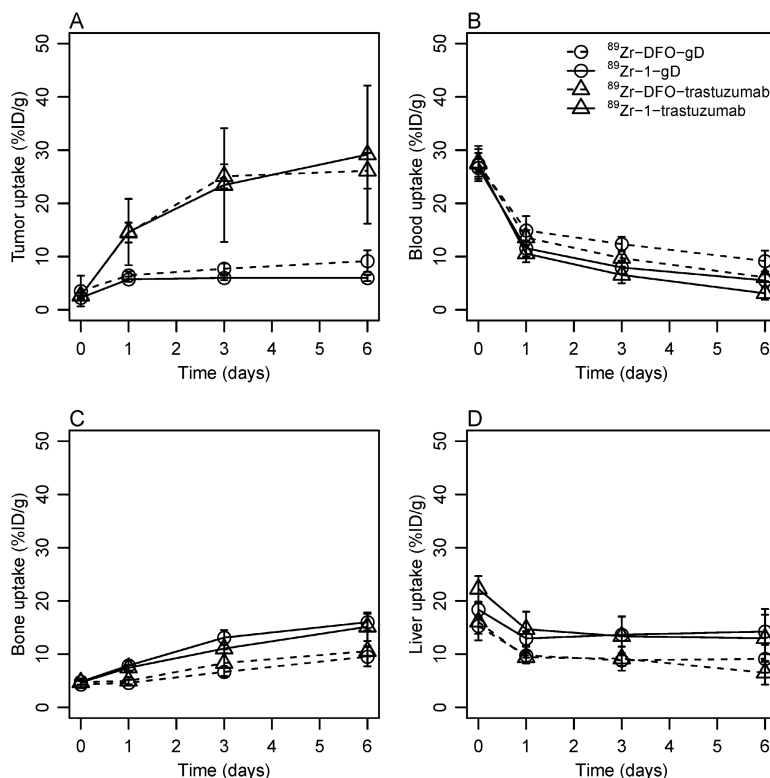


**Figure 2.** Uptake of  $^{89}\text{Zr}$ -labeled antibodies in SKOV3 xenograft, heart, bone and liver was determined by PET imaging of mice bearing SKOV3 tumors.



The elevated liver uptake of antibodies conjugated to **1** observed at 1 h p.i. was present through day 1, 3 and 6 but the slope of the time activity curve was parallel to the liver uptake of DFO labeled tracers supporting the hypothesis that the impurities present in  $^{89}\text{Zr}$ -**1**-trastuzumab and  $^{89}\text{Zr}$ -**1**-gD sequestered in liver and further hepatobiliary metabolism of both (**1**- and DFO-labeled) tracers proceeded at a similar rate. The liver uptake of trastuzumab derivatives remained roughly constant from day 1 to 6 (**Figure 2D**) with day 6 levels  $6.5 \pm 2.2$  %ID/g for  $^{89}\text{Zr}$ -DFO-trastuzumab compared to  $13.0 \pm 4.4$  %ID/g for **1**-trastuzumab ( $p = 0.01$ ). The liver uptake of **1**-gD and  $^{89}\text{Zr}$ -DFO-gD reached similar levels and followed the same trend as trastuzumab derived tracers.

The radioactivity uptake in bone reflects the extent of  $^{89}\text{Zr}$  release from the complex. The bone uptake measured in the hind leg knee was not different between  $^{89}\text{Zr}$ -DFO-gD and  $^{89}\text{Zr}$ -DFO-trastuzumab ( $p = 0.390, 0.388$  at days 1 and 6 p.i. respectively) or between  $^{89}\text{Zr}$ -**1**-gD and  $^{89}\text{Zr}$ -**1**-trastuzumab ( $p = 0.350, 0.474$ ). But it was significantly higher in groups imaged with  $^{89}\text{Zr}$ -**1**-labeled antibodies than in the groups imaged with  $^{89}\text{Zr}$ -DFO-labeled antibodies through day 1 to 6 p.i. (**Figure 2C**). The bone uptake in the group imaged with  $^{89}\text{Zr}$ -**1**-trastuzumab steadily increased and reached  $15.1 \pm 2.7$  %ID/g at day 6; it was significantly ( $p = 0.0003$ ) higher than the uptake of radioactivity in the bone tissue in the group imaged with  $^{89}\text{Zr}$ -DFO-trastuzumab ( $10.6 \pm 1.0$  %ID/g). The bone uptake in groups imaged with tracers derived from anti-gD antibody reached similar levels and followed similar trends with significantly ( $p = 4.6 \times 10^{-5}$ ) higher bone uptake in  $^{89}\text{Zr}$ -**1**-gD group than in  $^{89}\text{Zr}$ -DFO-gD group at day 6. The elevated bone uptake of  $^{89}\text{Zr}$  observed with tracers labeled using **1** compared to the tracers labeled using DFO in PET is in line with the limited stability of  $^{89}\text{Zr}$ -**1** and  $^{89}\text{Zr}$ -**1**-trastuzumab in serum (**Table S2, Figure S4**) and the elevated  $^{89}\text{Zr}$ -**1** bone uptake observed in biodistribution experiment (**Table S3**). Although a direct comparison has not been conducted, the bone uptake observed with  $^{89}\text{Zr}$ -**1**-labeled antibodies in this study appears to be lower than the uptake of  $^{89}\text{Zr}$ -YM103-trastuzumab [18]. Ma et al. reported that PET imaging in mice with  $^{89}\text{Zr}$ -YM103-trastuzumab resulted in  $25.9 \pm 0.6$  %ID/g bone uptake at day 7 p.i. which is higher than  $15.1 \pm 2.7$  %ID/g observed at day 6 p.i. in this study. Despite different conjugation chemistries that were used by Ma et al. and in our study, both studies used DFO as the standard  $^{89}\text{Zr}$  chelator. The normalization of the bone uptake of  $^{89}\text{Zr}$ -**1**-trastuzumab and  $^{89}\text{Zr}$ -YM103-trastuzumab to the bone  $^{89}\text{Zr}$ -DFO-trastuzumab allows comparison of the tracers. The ratio of bone uptake of

$^{89}\text{Zr}$ -YM103-trastuzumab and  $^{89}\text{Zr}$ -DFO-trastuzumab reported by Ma et al. was 4 at day 7 p.i. which is much higher than the same ratio observed in this study (1.4 at day 6). The comparison of normalized bone uptakes revealed much higher *in vivo* stability of  $^{89}\text{Zr}$ -antibodies labeled via bi-cyclic octadentate ligand **1** than the *in vivo* stability of  $^{89}\text{Zr}$ -antibodies labeled using tripodal hexadentate ligand CP256. The use of conformationally constrained octadentate HOPO-based ligands for  $^{89}\text{Zr}$  is clearly a step forward on the path to develop  $^{89}\text{Zr}$ -chelators superior to DFO. The effect of changing the scaffold topology responsible for positioning the 3,2-HOPO coordination units is the subject of current investigation.

Taken altogether, the impurities present in **1**-labeled antibodies likely contributed to the observed higher liver uptake and the elevated bone uptake observed in **1**-labeled antibodies was caused by lower stability of  $^{89}\text{Zr}$ -**1** complex compared to  $^{89}\text{Zr}$ -DFO complexes. Despite the lower purity and stability of **1** labeled antibodies the HER2-specific tumor uptakes of trastuzumab derived tracers were identical and the impact of lower stability and purity to overall image quality seems negligible (**Figure 3**).

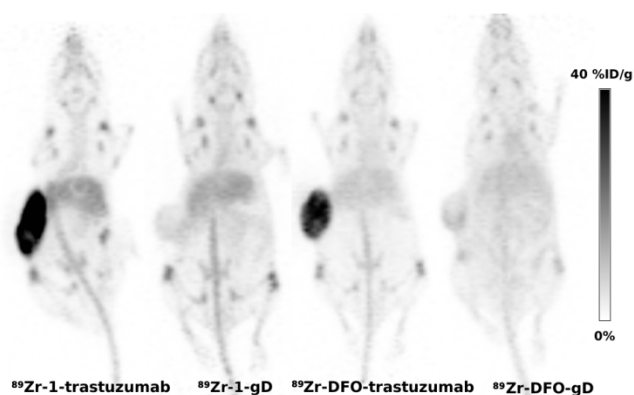


**Figure 3.** Representative PET images (maximum intensity projections) obtained using  $^{89}\text{Zr}$ -antibodies labeled by **1** and DFO and SKOV3 xenograft bearing mice at day 6 p.i.

## Conclusions

The complexes of  $\text{Zr}^{4+}$  with 3-hydroxypyridin-2-one based di-macrocylic ligand **1** were formed in 1:1 ratio and the quantitative chelation of  $^{89}\text{Zr}^{4+}$  was achieved under mild conditions within 15 minutes. The  $^{89}\text{Zr}$ -**1** was stable *in vitro* in presence of DTPA, but a slow degradation was observed in serum. *In vivo*, the hydrophilic  $^{89}\text{Zr}$ -**1** complex showed prevalently renal excretion; and an elevated bone uptake of radioactivity suggested a partial release of  $^{89}\text{Zr}^{4+}$  from the complex.

The di-macrocylic ligand **1** was conjugated to monoclonal antibodies, trastuzumab and anti-gD, using a p-phenylene bis-isothiocyanate linker to yield

products with an average loading of less than 2 molecules of **1** per antibody. The trastuzumab conjugate retained its binding affinity to HER2. Both antibodies were labeled with  $^{89}\text{Zr}$  under mild conditions providing the PET tracers in 60-69% yield and acceptable purity. Despite the limited stability of  $^{89}\text{Zr}$ -**1**-trastuzumab in mouse serum; the PET tracers performed very well *in vivo*. The PET imaging in mouse model of HER2 positive ovarian carcinoma showed tumor uptake of  $^{89}\text{Zr}$ -**1**-trastuzumab indistinguishable from the uptake of positive control  $^{89}\text{Zr}$ -DFO-trastuzumab; however, the non-specific uptake of  $^{89}\text{Zr}$ -**1** labeled tracers was slightly elevated in liver and bone compared to  $^{89}\text{Zr}$ -DFO based tracers.

In conclusion, the presented study demonstrated that the 3-hydroxypyridin-2-one based di-macrocyclic ligand **1** provides a viable alternative to DFO for immunoPET studies. An optimization of the macrocyclic scaffold in respect to positioning the 2,3-HOPO units and increase the *in-vivo* stability of the complexes is ongoing.

## Abbreviations

ESI-MS: Electrospray Ionization Mass Spectrometry; ITLC: Instant Thin Layer Chromatography; kBq: Kilobecquerel;  $K_D$ : Binding Constant; MBq: Megabecquerel; %/ID/g: Percent injected does per gram of tissue; p.i.: post-injection; ROI: Region of Interest; RU: Response Unit; SPR: Surface Plasmon Resonance; TLC: Thin Layer Chromatography, SEC HPLC: Size exclusion column HPLC, HER2: human epidermal growth factor receptor 2

## Supplementary Material

Synthetic protocols and analytical data for all compounds, *in vitro* stability data and *in vivo* biodistribution data for  $^{89}\text{Zr}$  complexes. Supplementary Tables and Figures.

<http://www.thno.org/v06p0511s1.pdf>

## Acknowledgements

$^{89}\text{Zr}$  was obtained with support from Department of Energy Office of Science, Nuclear Physics Isotope Program (DESC0008657).

## Grant support

This research was supported in part by NSF SBIR Phase I grant No. IIP-1215462 to Lumiphore, Inc. and Wake Forest University Health Sciences.

## Competing Interests

D. Magda and S. Pailloux are employees of Lumiphore, Inc., a company developing bi-functional metal chelators for commercial applications.

Other authors have declared that no competing interest exists.

## References

- van Dongen GA, Visser GW, Lub-de Hooge MN, de Vries EG, Perk LR. Immuno-PET: a navigator in monoclonal antibody development and applications. *The oncologist*. 2007; 12: 1379-89.
- Marik J, Junutula JR. Emerging role of immunoPET in receptor targeted cancer therapy. *Current drug delivery*. 2011; 8: 70-8.
- Wadas TJ, Wong EH, Weisman GR, Anderson CJ. Coordinating radiometals of copper, gallium, indium, yttrium, and zirconium for PET and SPECT imaging of disease. *Chemical reviews*. 2010; 110: 2858-902.
- Tinianow JN, Gill HS, Ogasawara A, Flores JE, Vanderbilt AN, Luis E, et al. Site-specifically  $^{89}\text{Zr}$ -labeled monoclonal antibodies for ImmunoPET. *Nuclear medicine and biology*. 2010; 37: 289-97.
- Perk LR, Vosjan MJ, Visser GW, Budde M, Jurek P, Kiefer GE, et al. p-Isothiocyanatobenzyl-desferrioxamine: a new bifunctional chelate for facile radiolabeling of monoclonal antibodies with zirconium-89 for immuno-PET imaging. *European journal of nuclear medicine and molecular imaging*. 2010; 37: 250-9.
- Verel I, Visser GW, Boellaard R, Stigter-van Walsum M, Snow GB, van Dongen GA.  $^{89}\text{Zr}$  immuno-PET: comprehensive procedures for the production of  $^{89}\text{Zr}$ -labeled monoclonal antibodies. *J Nucl Med*. 2003; 44: 1271-81.
- Holland JP, Divilov V, Bander NH, Smith-Jones PM, Larson SM, Lewis JS.  $^{89}\text{Zr}$ -DFO-591 for immunoPET of prostate-specific membrane antigen expression *in vivo*. *J Nucl Med*. 2010; 51: 1293-300.
- Fletcher CR. The radiological hazards of zirconium-95 and niobium-95. *Health physics*. 1969; 16: 209-20.
- Mealey J, Jr. [Turn-over of carrier-free zirconium-89 in man.]. *Nature*. 1957; 179: 673-4.
- Shiraishi Y, Ichikawa R. Absorption and retention of  $^{144}\text{Ce}$  and  $^{95}\text{Zr}$ -95 Nb in newborn, juvenile and adult rats. *Health physics*. 1972; 22: 373-8.
- Guerard F, Lee YS, Tripiet R, Szajek LP, Deschamps JR, Brechbiel MW. Investigation of Zr(IV) and  $^{89}\text{Zr}$ (IV) complexation with hydroxamates: progress towards designing a better chelator than desferrioxamine B for immuno-PET imaging. *Chem Commun (Camb)*. 2013; 49: 1002-4.
- Patra M, Bauman A, Mari C, Fischer CA, Blaque O, Haussinger D, et al. An octadentate bifunctional chelating agent for the development of stable zirconium-89 based molecular imaging probes. *Chem Commun (Camb)*. 2014; 50: 11523-5.
- Deri MA, Ponnala S, Zeglis BM, Pohl G, Dannenberg JJ, Lewis JS, et al. Alternative chelator for (89)Zr radiopharmaceuticals: radiolabeling and evaluation of 3,4,3-LI(1,2-HOPO). *Journal of medicinal chemistry*. 2014; 57: 4849-60.
- Gorden AE, Shuh DK, Tiedemann BE, Wilson RE, Xu J, Raymond KN. Sequestered plutonium: [Pu(IV)]5LiO(Me-3,2-HOPO)]2--the first structurally characterized plutonium hydroxypyridonate complex. *Chemistry*. 2005; 11: 2842-8.
- Gorden AE, Xu J, Raymond KN, Durbin P. Rational design of sequestering agents for plutonium and other actinides. *Chemical reviews*. 2003; 103: 4207-82.
- Datta A, Raymond KN. Gd-hydroxypyridinone (HOPO)-based high-relaxivity magnetic resonance imaging (MRI) contrast agents. *Accounts of chemical research*. 2009; 42: 938-47.
- Deri MA, Ponnala S, Kozlowski P, Burton-Pye BP, Cicek HT, Hu C, et al. p-SCN-Bn-HOPO: A Superior Bifunctional Chelator for (89)Zr ImmunoPET. *Bioconjugate chemistry*. 2015; 26: 2579-91.
- Ma MT, Meszaros LK, Paterson BM, Berry DJ, Cooper MS, Ma Y, et al. Tripodal tris(hydroxypyridinone) ligands for immunoconjugate PET imaging with  $^{89}\text{Zr}^{4+}$ : comparison with desferrioxamine-B. *Dalton Transactions*. 2014.
- Pandya DN, Pailloux S, Tatum D, Magda D, Wadas TJ. Di-macrocyclic terphenylamide ligands as chelators for the PET radionuclide zirconium-89. *Chem Commun (Camb)*. 2015; 51: 2301-3.
- Wadas TJ, Sherman CD, Miner JH, Duncan JR, Anderson CJ. The biodistribution of [ $^{153}\text{Gd}$ ]/Gd-labeled magnetic resonance contrast agents in a transgenic mouse model of renal failure differs greatly from control mice. *Magn Reson Med*. 2010; 64: 1274-80.
- Bao Q, Newport D, Chen M, Stout DB, Chatzioannou AF. Performance evaluation of the inveon dedicated PET preclinical tomograph based on the NEMA NU-4 standards. *Journal of nuclear medicine : official publication, Society of Nuclear Medicine*. 2009; 50: 401-8.
- Daumann LJ, Tatum DS, Snyder BE, Ni C, Law GL, Solomon EI, et al. New insights into structure and luminescence of Eu(III) and Sm(III) complexes of the 3,4,3-LI(1,2-HOPO) ligand. *J Am Chem Soc*. 2015; 137: 2816-9.
- Liu M, Wang J, Wu X, Wang E, Abergel RJ, Shuh DK, et al. Characterization, HPLC method development and impurity identification for 3,4,3-LI(1,2-HOPO), a potent actinide chelator for radionuclide decorporation. *J Pharm Biomed Anal*. 2015; 102: 443-9.
- Cabbiness DK, Margerum DW. Macrocyclic effect on stability of copper(II) tetramine complexes. *Journal of the American Chemical Society*. 1969; 91: 6540-1.
- Avdeef A. Physicochemical profiling (solubility, permeability and charge state). *Curr Top Med Chem*. 2001; 1: 277-351.

26. Avdeef A, Testa B. Physicochemical profiling in drug research: a brief survey of the state-of-the-art of experimental techniques. *Cell Mol Life Sci.* 2002; 59: 1681-9.
27. Mannhold R, van de Waterbeemd H. Substructure and whole molecule approaches for calculating log P. *J Comput Aided Mol Des.* 2001; 15: 337-54.
28. van de Waterbeemd H, Smith DA, Jones BC. Lipophilicity in PK design: methyl, ethyl, futile. *J Comput Aided Mol Des.* 2001; 15: 273-86.
29. Abou DS, Ku T, Smith-Jones PM. In vivo biodistribution and accumulation of <sup>89</sup>Zr in mice. *Nuclear medicine and biology.* 2011; 38: 675-81.
30. Holland JP, Divilov V, Bander NH, Smith-Jones PM, Larson SM, Lewis JS. <sup>89</sup>Zr-DFO-J591 for immunoPET of prostate-specific membrane antigen expression in vivo. *J Nucl Med.* 2010; 51: 1293-300.
31. Pandit-Taskar N, O'Donoghue JA, Beylertgil V, Lyashchenko S, Ruan S, Solomon SB, et al. Zr-huJ591 immuno-PET imaging in patients with advanced metastatic prostate cancer. *European journal of nuclear medicine and molecular imaging.* 2014.
32. Bostrom J, Haber L, Koenig P, Kelley RF, Fuh G. High affinity antigen recognition of the dual specific variants of herceptin is entropy-driven in spite of structural plasticity. *PLoS one.* 2011; 6: e17887.